A High-Precision Offset Frequency Locking Technique With Delay Line Reference and AOM-Based Compensation

Xing Chen, Qian Liu, Yusheng Wang, Fei Meng, and Bin Luo

***Abstract*—We demonstrate a high-precision, high robustness frequency offset locking method,which made the frequency offset between mode-locked laser and continuous-wave laser below less than 3 Hz.The coarse frequency lock control is realized by the feedback control of PZT with electrical delay line as the reference. The fine frequency compensation is realized by feed-forward control of an acousto-optic modulator. The fractional frequency instability was 7.4×10^{-10} for an averaging time of 1 s, 3.3×10^{-8} for an averaging time of 10 000 s when the narrow linewidth laser is free-running. In this experiment, the fractional frequency instability can be achieved at 1.1×10^{-15} for an averaging time of 1 s, at 3.6×10^{-18} for an averaging time of 10 000 s when the system is fine frequency locked. Compared with the unlocked laser, the fractional frequency instability can be improved about 5–6 orders of magnitude. This work lays the foundation for simple structure, high robustness and high precision laser frequency control situation, such as quantum precision measurement and optical lattice clocks.**

***Index Terms*—Laser frequency stabilization, electrical delay line frequency stabilization, frequency offset locking.**

I. Introduction

FREQUENCY-stabilized lasers are applied in not only precision metrology fields [1]–[3] but also in advanced spectroscopy laboratories [4], astronomy [5], [6] and very long baseline interferometry [7]–[9], telecommunications industries [10], measurement of basic physical parameters [11]–[14], gravitational wave detection [15], low-noise microwave signal generation [16]–[18] and optical clock comparison [19]–[21]. Optical atomic clocks can realize high-precision and accuracy timekeeping and provide an accurate quantum frequency standard. Optical clocks, which have a narrow intrinsic linewidth and a stable center frequency laser, are aiming for the next-generation redefinition of the "second". Optical frequency comb (OFC) can convert optical clocks to 1550 nm wave band, which is the communication wave band the optical clocks rarely transferred in. And OFC is also used to transfer optical clocks in microwave band. Atomic and molecular resonances or stable optical cavities are used as frequency references to realize laser frequency stabilization. OFC delivered by optical fibers, which can obtain arbitrary or multiple optical frequencies in remote sites, paves the way for a ubiquitous optical reference network. Yusuke Hisai, Kohei Ikeda, etc. realized the frequency offset locking between two solid-state lasers by using an electrical delay line [22]. The frequency offset of the two lasers was successfully controlled within 23 kHz. The instability was 8.2×10^{-11} for an averaging time of 1 s. Compared with this method above, we have improved the instability by 5∼6 orders of magnitude. In this study, we demonstrate a high-precision, high-robust frequency offset locking method. The frequency offset locking between two 1550 nm lasers, including mode-locked laser (MLL) and narrow linewidth laser (NLL), is realized by electrical delay line and acousto-optic modulator (AOM). We demonstrate a stable frequency locking method for the transmission of optical signals. The electrical delay line is used to realize coarse frequency lock control by feedback control technology. The AOM is used to realize fine frequency compensation by feedforward control technology. As a result, the frequency offset locking between two 1550 nm lasers has a relative frequency instability of 1.1×10^{-15} at an averaging time of 1 s (corresponding to an absolute frequency less than 3 Hz) and 3.6×10^{-18} at an averaging time of 10 000 s. This laser could be employed as a pump laser for wavelength conversion in long-distance quantum communication. This work has a strong attraction for quantum measurement and precision frequency metrology.

II. Experiment

The control link is divided into two parts, namely feedback coarse frequency lock control and feed-forward fine frequency compensation. In feedback coarse frequency lock control module, where the frequency offset locking is less than 30 kHz, electrical delay line and proportional-integral control (PI) is used to lock the frequency. In feedforward fine frequency compensation module, where the frequency offset locking is less than 3 Hz, AOM is used to realize fast offset compensated between two lasers. By these two-step frequency offset locking, the frequency of NLL can be changed to follow the frequency of MLL. Thus,

Manuscript received August 5, 2021; accepted August 6, 2021. Date of publication August 10, 2021; date of current version August 27, 2021. This work was supported in part by the Youth Program of the National Natural Science Foundation of China (NSFC) under Grant 61901046, and in part by the Fundamental Research Funds for the Central Universities under Grants 2019PTB-004 and 2019XD-A18. *(Corresponding authors: Fei Meng; Bin Luo.)*

Xing Chen, Qian Liu, Yusheng Wang, and Bin Luo are with the State Key Laboratory of Information Photonics and Optical Communications, School of Electronic Engineering, Beijing University of Posts and Telecommunications, Beijing 100876, China (e-mail: chenxing@bupt.edu.cn; LiuQ@bupt.edu.cn; WangYusheng@bupt.edu.cn; luobin@bupt.edu.cn).

Fei Meng is with the Division of Time and Frequency Metrology, National Institute of Metrology, Beijing 100029, China (e-mail: mfei@nim.ac.cn).

Digital Object Identifier 10.1109/JPHOT.2021.3103659

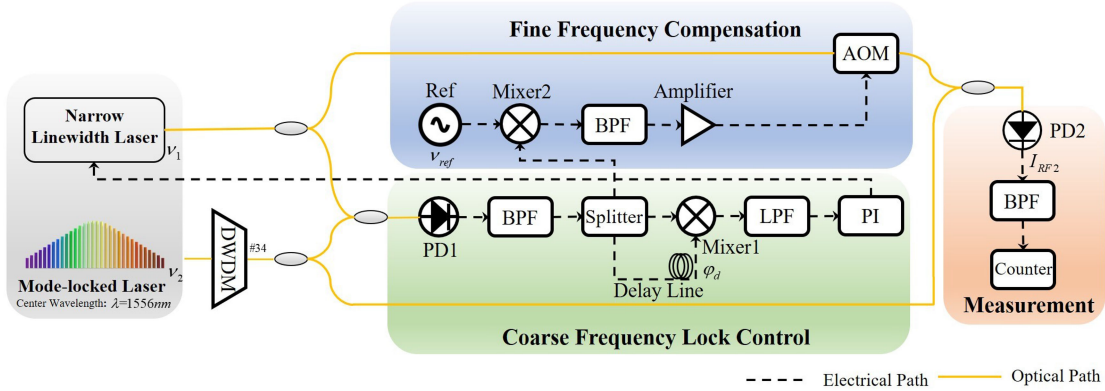

Fig. 1. Schematic diagram of frequency locking between NLL and MLL. PD: photo detector, LPF: Low Pass Filter, AOM: acousto-optic modulator, PI: proportional-integral control.

it can achieve high-precision optical frequency offset locking between the NLL and MLL. The principle is shown in Fig. 1.

Fig. 1. shows the schematic diagram of frequency locking between NLL and MLL. The MLL (MenloSystems, FC1550-250), which has a repetition frequency of 250 MHz, is used as the OFC source. The output power of MLL is 10.7 mW, and its center wavelength is 1541.2 nm, full width at half maximum is 129.7 nm. The output power of NLL (NKT X15) is 24.4 mW. A Channel #34 of Dense wavelength division multiplexing (DWDM) that center wavelength is 1550.14 nm and full width at half maximum is 0.8 nm, is used to filter the OFC signal generated by MLL. The beam is divided into two parts. One branch is coupled with NLL and transferred into feedback coarse frequency lock control module. In this branch, an error signal is obtained by delay line and feedback controlled by PI. The signal of another branch, which is coupled with NLL by AOM operating at 35 MHz, realizes feed-forward fine frequency compensated. Two beat frequency signals are obtained between NLL and MLL, by a three ports coupler with the splitting ratio of 50: 50. We assume the combined phase fluctuation between two lasers as φ_{laser}. The frequencies of the two beams are and, respectively. In the following discussion, $|\nu_1 - \nu_2|$ is expressed as $\Delta\nu$ and corresponds to the beat frequency. In coarse frequency lock module, the beat signal is divided into three signals by the power splitter. One signal is directly introduced into the mixer, which is proportional to $\cos(\Delta\nu t + \varphi_{laser})$. One signal is delayed by a 2-m-long coaxial cable, which is proportional to $\cos(\Delta\nu t + \varphi_d + \varphi_{laser})$. And another signal is mixed with an external reference source. As a function of the beat frequency offset ($\Delta\nu$) between two lasers, the beat frequency signal varies as $\cos\varphi_d$, where the phase shift φ_d introduced by the coaxial cable is $\varphi_d = \Delta\nu\tau_c$, and τ_c is the time delay introduced by the coaxial cable, which is calculated to be 10 ns for the 2-m-long cable ($\tau_c \approx 5$ ns for a cable of 1 m length) [23]. The servo error signal M_1 from mixer1 is

$$\begin{aligned} M_1 &\propto \cos(\Delta\nu t + \varphi_{laser})\cos(\Delta\nu t + \varphi_d + \varphi_{laser}) \\ &= \cos(\nu_1 t - \nu_2 t + \varphi_{laser})\cos(\nu_1 t - \nu_2 t + \varphi_d + \varphi_{laser}) \\ &\approx \cos(\nu_1 t + \varphi_{laser})\cos(\nu_2 t)\cos(\nu_1 t - \nu_2 t + \varphi_d + \varphi_{laser}) \\ &\approx \cos(\varphi_d) + \cos(2\Delta\nu t + \varphi_d + 2\varphi_{laser}) \end{aligned} \quad (1)$$

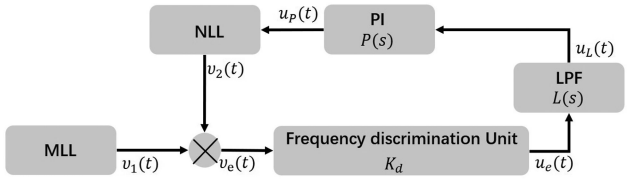

Fig. 2. Simplified configuration of coarse frequency control module.

The alternating current component $\cos(2\Delta\nu t + \varphi_d + 2\varphi_{laser})$ in (1) can be filtered by a low pass filter (LPF). As a result, the error signal is obtained as

$$M_1 \propto \cos(\varphi_d) = \cos(\Delta\nu\tau_c) \quad (2)$$

The delay line is used as the external reference source [24]. The output of the mixer1 provides information about the frequency offset between the two signals. The PI is used to realize the feedback control of the NLL. The coarse frequency locking can be realized and the frequency offset between MLL and NLL is suppressed from ~70 MHz to ~30 kHz.

In the coarse frequency locking control module, in order to analyze the frequency-locked performance, we construct a mathematical model of phase locked loop (PLL) in Fig. 2. And the analysis is performed in frequency domain using Laplace transform. The open-loop transfer function $G(s)$, the close-loop transfer function $H(s)$, and the error-transfer function $H_e(s)$ is given as follow.

$$G(s) = \frac{V_2(s)}{V_e(s)} = K_d L(s) P(s) \quad (3)$$

$$H(s) = \frac{V_2(s)}{V_1(s)} = \frac{K_d L(s) P(s)}{1 + K_d L(s) P(s)} \quad (4)$$

$$H_e(s) = \frac{V_e(s)}{V_1(s)} = \frac{1}{1 + K_d L(s) P(s)} \quad (5)$$

where $\nu_1(t)$ and $\nu_2(t)$ are the frequency of MLL and NLL respectively, $\nu_e(t)$ is the beat frequency of MLL and NLL. $V_1(s)$, $V_2(s)$ and $V_e(s)$ are the Laplace transforms of $\nu_1(t)$, $\nu_2(t)$ and $\nu_e(t)$ respectively. $K_d = 10$ mV/MHz is the phase sensitivity of the frequency discrimination unit, $u_e(t)$ is the frequency discrimination error signal, $u_L(t)$ is the filtered signal after the

loop filter, $u_P(t)$ is the deviation control by the PI controller to compensate for phase noise.

The transfer function of the loop filter is given by

$$L(s) = \frac{1}{1 + s \cdot \tau} \tag{6}$$

where $\tau = 0.084\ \mu$s is the time constant of LPF.

The transfer function $P(s)$ of PI controller is given by

$$P(s) = \frac{U_P(s)}{U_L(s)} = K_P + K_I/s \tag{7}$$

where $K_P = 25$ dB is the proportional coefficient and $K_I = K_P/T_i = K_P \times 2\pi \times 300$ Hz $= 47$ dB $\cdot$ kHz (the corner frequency of PI is 300 Hz) is the integral time constant, respectively.

In order to further improve the accuracy of the locking, we lock the output signal of the coarse frequency locking control module with the reference frequency source, which can effectively suppress the phase noise between two signals. AOM is used to compensate for the system noise [25]. One of the beat signals, which is coarse locked, is mixed with an external reference source (ν_{Ref}). The mixed signal is filtered, amplified and then enters the modulator unit, where the feedback control of AOM is realized. The drive signal for AOM, M_2, is

$$\begin{aligned} M_2 &\propto \cos\left(\Delta\nu t + \varphi_{laser}\right)\cos\left(\nu_{Ref} t\right) \\ &\approx \frac{1}{2}\cos\left(\Delta\nu t - \nu_{Ref} t + \varphi_{laser}\right) \end{aligned} \tag{8}$$

Finally, the beat-frequency signal is obtained by the mixing of the signal and the NLL compensated by AOM, and the fine frequency compensation can be realized. A RF signal intensity, I_{RF_2}, generated by PD2 can be obtained as

$$\begin{aligned} I_{RF_2} &\propto \cos\left[\left(\nu_1 + \Delta\nu - \nu_{\mathrm{Ref}}\right)t + \varphi_{laser}\right]\cos\left(\nu_2 t + \varphi_{laser}\right) \\ &= \frac{1}{2}\left\{\cos\left(\nu_{Ref} t\right) + \cos\left[\left(\nu_1 + \nu_2 + \Delta\nu - \nu_{Ref}\right)t\right.\right. \\ &\quad \left.\left. -2\varphi_{laser}\right]\right\} \\ &\approx \frac{1}{2}\cos\left(\nu_{Ref} t\right) \end{aligned} \tag{9}$$

By the fine frequency compensation module, we can eliminate the phase fluctuation of the laser, the phase noise caused by the fiber link and other phase noise. The frequency offset between MLL and NLL is suppressed from ~30 kHz to ~3 Hz.

III. Results

We evaluated the instability of the frequency offset between NLL and MLL. A frequency counter (Keysight 53230 A) employed to measure the offset frequency, ant its gate time set as 1 s. We tested the results of the frequency offset when the NLL is free running, coarse frequency locking and fine frequency compensation. When locked, the frequency difference between the lasers is about 27 MHz. Fig. 3(a). shows the variation in frequency offset when NLL was free running is about 70 MHz in 55 000 s. Fig. 3(b). shows when NLL was coarse frequency locking, the variation in frequency offset is about 30 kHz in

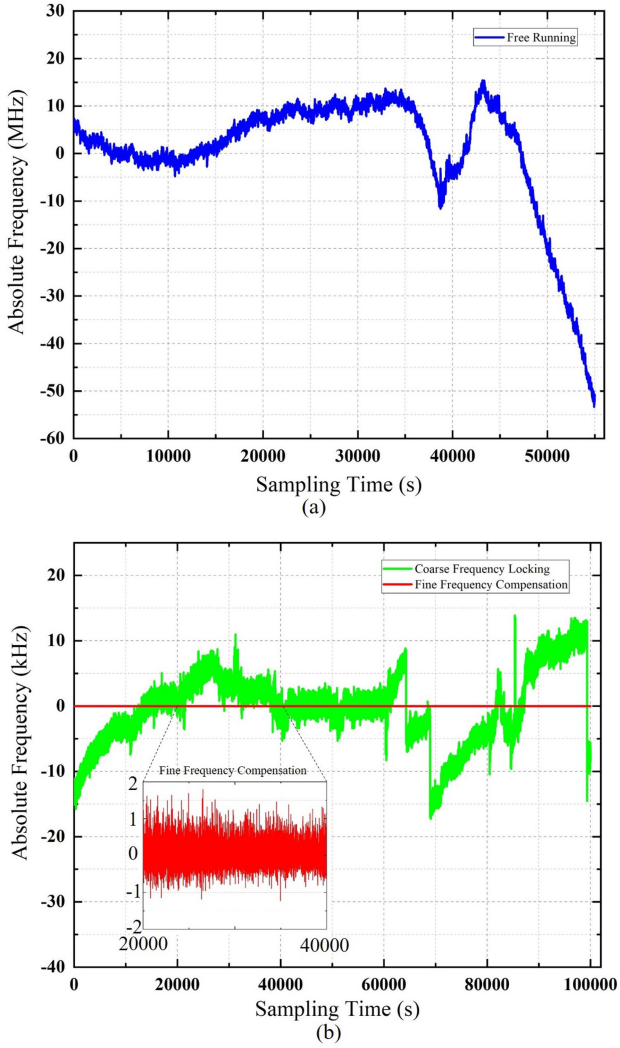

Fig. 3. Comparison of variation in the frequency offset between two lasers, when NLL was free running, coarse frequency locking (without AOM compensation) or fine frequency compensation (with AOM compensation). Indicated data are the frequency offset when NLL was (a) free running (blue trace); (b) coarse frequency locking (green trace) and fine frequency compensation (red trace).

100 000 s and when NLL was fine frequency compensation, the variation in frequency offset is about 3 Hz in 100 000 s, and we intercepted a part of 20 000 s shown in the detailed figure. The frequency offset locking method completes the high-precision frequency locking experiment with MLL and NLL. The variation in frequency offset between NLL and MLL is suppressed within 3 Hz.

Fig. 4. shows Allan deviation of the variation in frequency offset between two lasers. The fractional frequency instability was 7.4×10^{-10} for an averaging time of 1 s, after an averaging time of 10 000 s was increasing towards 3.3×10^{-8} when NLL is free running. The fractional frequency instability was 2.6×10^{-12} for an averaging time of 1 s, after an averaging time of 10 000 s was increasing towards 2.0×10^{-11} when NLL is coarse frequency locking. Compared with the fractional frequency instability when NLL is free running, the fractional frequency instability of coarse frequency locking was improved

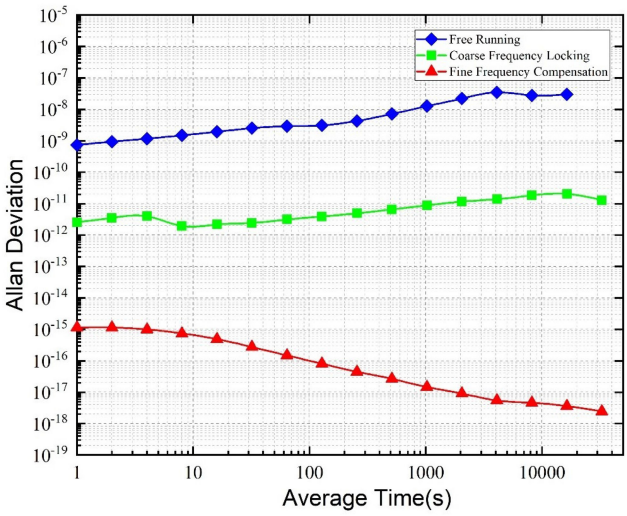

Fig. 4. Fractional frequency instability of the beat frequency between the two lasers, when NLL was free running (blue trace), coarse frequency locking (green trace), and fine frequency compensation (red trace).

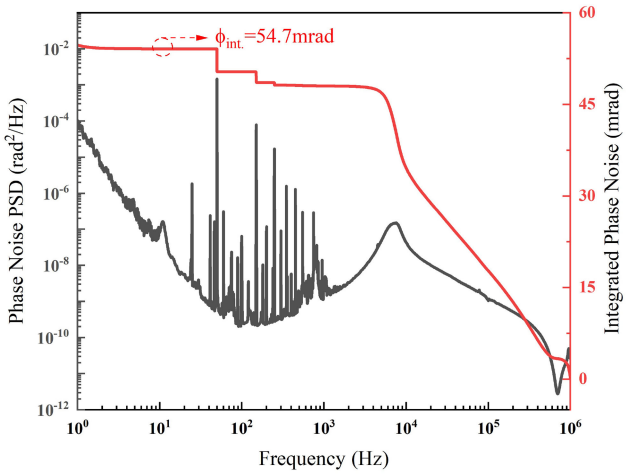

Fig. 5. The power spectral density of phase noise in fine frequency compensation module. Black curve is power spectral density, red curve is integrated phase noise, red dashed line is the residual in-loop integrated phase noise.

approximately 2∼3 orders of magnitude. The fractional frequency instability was 1.1×10^{-15} for an averaging time of 1 s, after an averaging time of 10 000 s was increasing towards 3.6×10^{-18} when NLL is fine frequency compensation. Compared with coarse frequency locking, the fractional frequency instability of fine frequency compensation is improved approximately 3∼4 orders of magnitude.

We mearused the phase noise power spectral density of fine frequency compensation. Fig. 5. shows the phase noise in fine frequency compensation module. Phase noise analyzer (5125, Microsemi) is used to measure the phase noise of the frequency offset. 10 MHz H-maser is used as a reference. When Fourier frequency is 1 Hz, the power of spectral density is less than $10^{-4} rad^2$/Hz. The integrated phase noise radian is 54.70 mrad from 1 Hz to 1 MHz. The steep drop in integrated phase noise curve is caused by the 50 Hz power frequency and it harmonic wave.

TABLE I
COMPARISON OF THE FREQUENCY OFFSET LOCKING TECHNOLOGY

Works	Frequency Fluctuations	The Frequency Instability 1 s	The Frequency Instability 1,000 s
Ref. [23]	Below 1 MHz @ 1 h	-	-
Ref. [26]	Below 1 kHz @ 1 s	-	-
Ref. [27]	Below 1 kHz @ 20 s	-	-
Ref. [28]	Above 1 MHz @ 20 s	-	-
Ref. [29]	-	7×10^{-14}	$\sim 7 \times 10^{-14}$
Ref. [30]	-	8.4×10^{-12}	$\sim 1 \times 10^{-14}$
This work	Below 3 Hz @ 100,000 s	1.1×10^{-15}	1.4×10^{-17}

Table I has summarized the typical recent reports of the frequency offset locking technology. This table shows that our method has high robustness, low residual frequency fluctuation and long frequency locking time.

IV. CONCLUSION

In this paper, we demonstrate a novel frequency-locking method for the high robustness, high-precision frequency offset locking between MLL and NLL. We use an electrical delay-line as a frequency reference to improve the fractional frequency instability to 2.6×10^{-12} for an averaging time of 1 s, and use AOM to improve the fractional frequency instability to 1.1×10^{-15} for an averaging time of 1 s. Compared with the fractional frequency instability when NLL is free running, the fractional frequency instability can be improved about 5∼6 orders of magnitude when the laser is fine frequency compensation. The test result is shown that the frequency offset between MLL and NLL is less than 3 Hz, the locking time between two lasers is more than 100 000 s. The fractional frequency instability of fine frequency compensation can be achieved at 3.6×10^{-18} for an averaging time of 10 000 s.

Using a MLL, the signal could be locked at arbitrary frequency of optical frequency comb. The frequency reference could be transferred by optical fiber and the frequency of laser could be locked at remote site. Compared with the phase locking method, this frequency offset locking with delay line reference and AOM-based compensation method has high robustness, and the frequency offset can be locked in high dynamic range (∼dozens of megahertz). In the meanwhile, a relatively slow servo component can be used merely rather than a high-speed and complex phase-locked circuit, which is simple and low-cost. If acousto-optic devices are used with feedforward technology, the high accuracy and phase noise performance, which phase-locked technology achieves, could be realized. This technique can be applied to optical lattice clocks, quantum communication and precision frequency metrology.

APPENDIX
EVALUATION OF SYSTEM STABILIZATION

In this method, the frequency stability is greatly improved by feedback control and feedforward control. We have evaluated the factors influenced the stability of this frequency locking system.

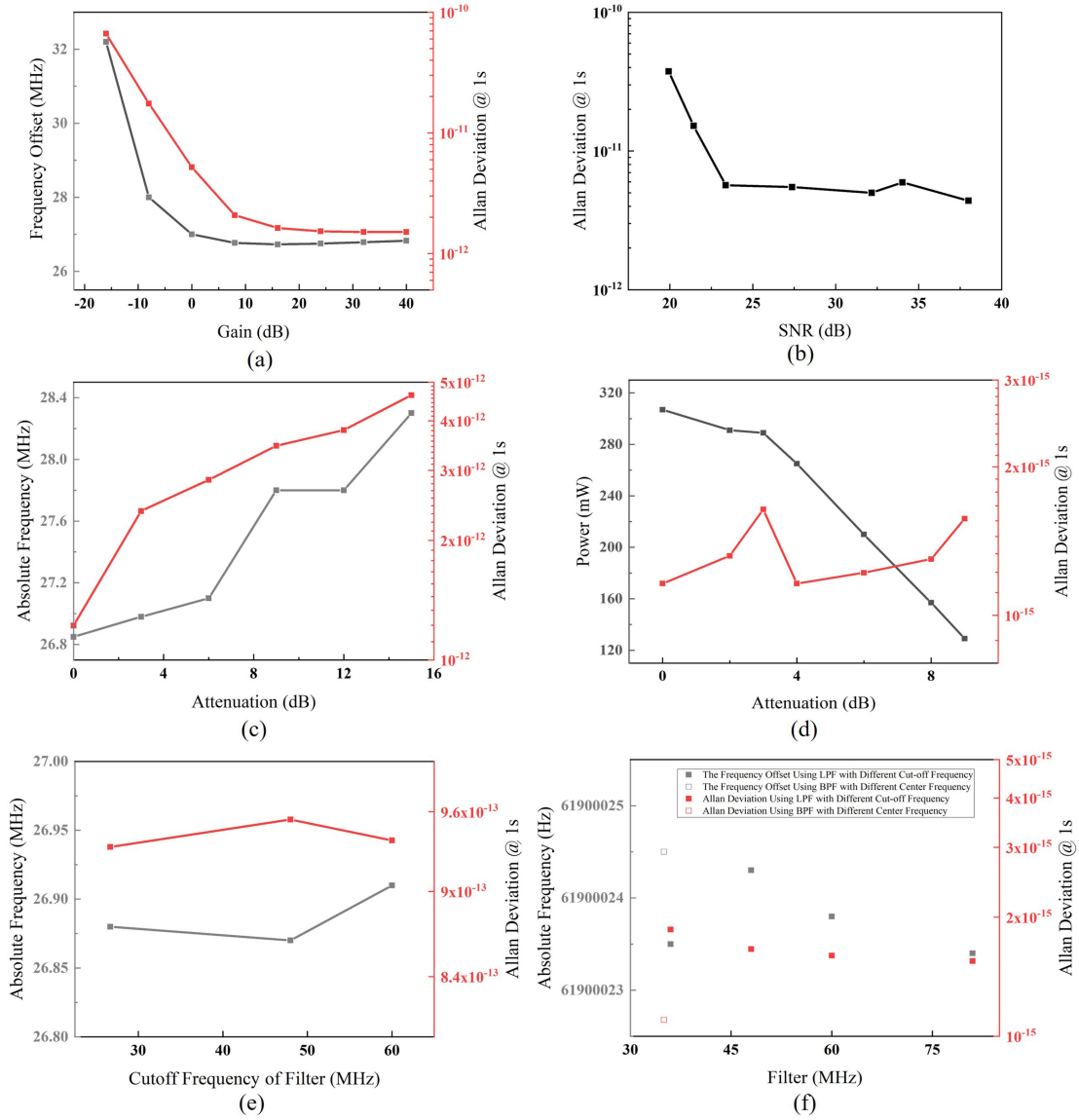

Fig. 6. The evaluation of factors influenced the frequency stability. The factors include: (a) servo gain of PI controller, (b) SNR of input signal of delay line, (c) input signal power of delay line, (d) the electrical power of the beat signal before AOM, (e) BPF after PD1 is changed to LPF with different cut-off frequency, (f) BPF after Mixer2 is changed to different types of filters.

We performed a series of quantitative study to evaluate how these factors affect the stability in Fig. 6.

Fig. 6(a). shows that when we improve the servo gain of PI controller, the frequency instability improves and the frequency offset decreases. The PI controller used in this method is LB1005, and its servo gain is continuously adjusted by the 10-turn knob. The gain of the loop filter is from -40 dB (fully counter clockwise) to +40 dB (fully clockwise). When the servo gain is below 8 dB, the instability descends and until servo gain is less than -16 dB, the frequency offset can not be locked. When the servo gain is over 8 dB, the system has better frequency stabilization. The gain setting in this method is 24 dB. Fig. 6(b). shows the SNR of input signal of delay line. The minimum SNR required in this method is 23 dB. When SNR improves over 23 dB, the frequency instability can maintain at the level $\sim 5 \times 10^{-12}$ (resolution bandwidth, RBW, of 100 kHz). Fig. 6(c). shows the input signal power of delay line is inversely related to frequency instability. The power decreases, the instability descends and the frequency offset decreases. The input power in this method is 6.83 dBm with the frequency instability at 1.22×10^{-12}. Fig. 6(d). shows when we reduce the electrical power of the beat signal before AOM, the instability changes at the level $\sim 1 \times 10^{-15}$. As shown in Fig. 6(e). and Fig. 6(f), the influence can be ignored with enough SNR when the BPF after PD1 and BPF after Mixer2 are changed, respectively.

REFERENCES

[1] J. Kodet, P. Pánek, and I. Procházka, "Two-way time transfer via optical fiber providing subpicosecond precision and high temperature stability," *Metrologia*, vol. 53, no. 1, pp. 18–26, 2016.

[2] Z. Jiang, A. Czubla, J. Nawrocki, W. Lewandowski, and E. F. Arias, "Comparing a GPS time link calibration with an optical fiber self-calibration with 200 ps accuracy," *Metrologia*, vol. 52, no. 2, pp. 384–391, 2015.

[3] M. Rost, D. Piester, W. Yang, T. Feldmann, T. Wübbena, and A. Bauch, "Time transfer through optical fibers over a distance of 73 km with an uncertainty below 100 ps," *Metrologia*, vol. 49, no. 6, pp. 772–778, 2012.

[4] P. Morzynski *et al.*, "Absolute measurement of the 1S0-3P0 clock transition in neutral 88Sr over the 330 km-long stabilized fiber optic link," *Sci. Rep*., vol. 5, 2015, Art. no. 17495.

[5] S. W. Schediwy, D. R. Gozzard, S. Stobie, J. A. Malan, and K. Grainge, "Stabilized microwave-frequency transfer using optical phase sensing and actuation," *Opt. Lett*., vol. 42, no. 9, pp. 1648–1651, 2017.

[6] B. Wang, X. Zhu, C. Gao1, Y. Bai1, J. W. Dong, and L. J. Wang, "Square kilometer array telescope-precision reference frequency synchronization via 1f-2f dissemination," *Sci. Rep.*, vol. 5, 2015, Art. no. 13851.

[7] C. Clivati *et al.*, "A VLBI experiment using a remote atomic clock via a coherent fiber link," *Sci. Rep.*, vol. 7, 2017, Art. no. 40992.

[8] P. Krehlik *et al.*, "Fiber-optic delivery of time and frequency to VLBI station," *Astron. Astrophys*., vol. 603, no. A48, pp. 1–8, 2017.

[9] E. F. Dierikx *et al.*, "White rabbit precision time protocol on long distance fiber links," *IEEE Trans. Ultrason. Ferroelectr. Freq. Control*, vol. 63, no. 7, pp. 945–952, Jul. 2016.

[10] Ł. Śliwczyński *et al.*, "Fiber-optic time transfer for UTC-traceable synchronization for telecom networks," *IEEE Commun. Standards Mag.*, vol. 1, no. 1, pp. 66–73, Mar. 2017.

[11] K. L. Corwin, Z. T. Lu, C. F. Hand, R. J. Epstein, and C. E. Wieman, "Frequency-stabilized diode laser with the Zeeman shift in an atomic vapor," *Appl. Opt.*, vol. 37, no. 15, pp. 3295–3298, 1998.

[12] H. Metcalf and P. V. D. Straten, "Cooling and trapping of neutral atoms," *Phys. Rep.*, vol. 244, no. 4-5, pp. 203–285, 1994.

[13] H. Müller *et al.*, "Tests of relativity by complementary rotating Michelson-Morley experiments," *Phys. Rev. Lett.*, vol. 99, no. 5, 2007, Art. no. 0 50401.

[14] S. G. Turyshev, "Experimental tests of general relativity: Recent progress and future directions," *Phys.-Usp.*, vol. 52, no. 1, pp. 1–27, 2009.

[15] S. J. Waldman, "Status of LIGO at the start of the fifth science run," *Classical Quantum Gravity*, vol. 23, no. 19, pp. S653–S660, 2006.

[16] J. Millo *et al.*, "Ultra-low noise microwave generation with fiber-based optical frequency comb and application to atomic fountain clock," *Appl. Phys. Lett.*, vol. 94, no. 14, pp. 1–3, 2009.

[17] A. Bartels *et al.*, "Femtosecond-laser-based synthesis of ultrastable microwave signals from optical frequency references," *Opt. Lett.*, vol. 30, no. 6, pp. 667–669, 2005.

[18] T. M. Fortier *et al.*, "Generation of ultrastable microwaves via optical frequency division," *Nat. Photon.*, vol. 5, pp. 425–429, 2011.

[19] M. M. Boyd *et al.*, "Optical atomic coherence at the 1-second time scale," *Science*, vol. 314, no. 5804, pp. 1430–1433, 2006.

[20] A. D. Ludlow *et al.*, "Sr lattice clock at 1×10^{-16} fractional uncertainty by remote optical evaluation with a Ca clock," *Science*, vol. 319, no. 5871, pp. 1805–1808, 2008.

[21] T. Rosenband *et al.*, "Frequency ratio of Al^{+} and Hg^{+} single-ion optical clocks," *Science*, vol. 319, no. 5871, pp. 1808–1812, 2008.

[22] Y. Hisai *et al.*, "Evaluation of laser frequency offset locking using an electrical delay line," *Appl. Opt.*, vol. 57, no. 20, pp. 5628–5634, 2018.

[23] U. Schunemann, H. Engler, R. Grimm, M. Weidemuller, and M. Zielonkowski, "Simple scheme for tunable frequency offset locking of two lasers," *Rev. Sci. Instrum.*, vol. 70, no. 1, pp. 242–243, 1999.

[24] K. Komori, Y. Takasu, M. Kumakura, Y. Takahashi, and T. Yabuzaki, "Injection-locking of blue laser diodes and its application to the laser cooling of neutral ytterbium atoms," *Jpn. J. Appl. Phys.*, vol. 42, no. 8, pp. 5059–5062, 2003.

[25] Z. T. Feng *et al.*, "Ultra-low noise optical injection locking amplifier with AOM-based coherent detection scheme," *Sci. Rep.*, vol. 8, 2018, Art. no. 13135.

[26] D. Bodenmüller, J. M. C. Boggio, M. M. Roth, and D. Bodenmuller, "Frequency offset stabilization for frequency combs using electro-optic modulators," in *Proc. AP*, Burlingame, CA, USA, 2019, pp. JT4A.2.

[27] G. Ritt, G. Cennini, C. Geckeler, and M. Weitz, "Laser frequency offset locking using a side of filter technique," *Appl. Phys. B.*, vol. 79, no. 3, pp. 363–365, 2004.

[28] T. Uehara, K. Tsuji, K. Hagiwara, and N. Onodera, "Optical beat-note frequency stabilization between two lasers using a radio frequency interferometer in the gigahertz frequency band," *Opt. Eng*. vol. 53, no. 12, 2014, Art. no. 124109.

[29] F. C. Reynolds and J. J. Mcferran, "Optical frequency stabilization with a synchronous frequency-to-voltage converte," *Appl. Opt.*, vol. 58, no. 12, pp. 3128–3132, 2019.

[30] D. A. Tulchinsky, "Sub 23 uHz instantaneous linewidth and frequency stability measurements of the beat note from an offset phase locked single frequency heterodyned Nd:YAG laser system," *Opt. Exp.*, vol. 25, no. 20, pp. 24119–24137, 2017.